ELSEVIER

Applied Surface Science 99 (1996) 185–196

applied surface science

Time-of-flight SIMS study of Bi–Mo selective oxidation catalysts

L.T. Weng [a,1], P. Bertrand [a,*], O. Tirions [b], M. Devillers [b,2]

[a] *Unité de Physico-Chimie et de Physique des Matériaux, Université Catholique de Louvain, Place Croix du Sud 1, B-1348 Louvain-la-Neuve, Belgium*

[b] *Laboratoire de Chimie Inorganique et Analytique, Université Catholique de Louvain, Place Croix du Sud 1, B-1348 Louvain-la-Neuve, Belgium*

Received 20 July 1995; accepted 21 January 1996

Abstract

The potential applicability of time-of-flight secondary ion mass spectrometry (TOF SIMS) to control the various stages of preparation of silica-supported Bi–Mo selective oxidation catalysts has been studied. These catalysts were prepared from coordination compounds (bismuth(III) and molybdenum(II) acetates or benzoates) as precursors. It has been shown that: (1) through the observation of the molecular ions and most characteristic fragments of the coordination compounds, TOF SIMS can provide direct information about the preservation of these precursors on the silica surface before calcination. (2) as the three pure bismuth molybdate phases (α-$Bi_2Mo_3O_{12}$, β-$Bi_2Mo_2O_9$ and γ-Bi_2MoO_6) show the same fragmentation patterns in TOF SIMS, they can only be distinguished in a indirect way, namely by comparing some SIMS intensity ratios from their positive spectra. These SIMS intensity ratios have been successfully used to determine the nature of bismuth molybdate phases formed on silica surface. And (3) TOF SIMS imaging provides valuable information about the dispersion of bismuth molybdate phase on silica surface.

Keywords: TOF SIMS; Coordination compounds; Bismuth molybdate; Selective oxidation

1. Introduction

Silica-supported bismuth molybdates are among the most important catalysts for the selective oxidation of olefins. They are classically prepared by an impregnation procedure from highly acidic aqueous solutions of bismuth(III) and molybdenum(VI) inorganic salts. In general, this method does not allow the adequate control of dispersion and nature of the formed phases, especially when complex multicomponent or multiphasic systems are generated. This is mainly due to non-uniform precursor–support interactions, as a consequence of the complex pattern of hydrolysis processes that occur in aqueous solution; these equilibria generate numerous polycationic ($[Bi_xO_y(OH)_z]^{n+}$) or polyanionic ($[Mo_xO_y]^{z-}$)

* Corresponding author. Tel.: +32-10-473581; fax: +32-10-473452; e-mail: bertrand@pcpm.ucl.ac.be.

[1] Present address: Materials Characterisation and Preparation Centre, The Hong Kong University of Science and Technology, Clear Water Bay, Kowloon, Hong Kong.

[2] Research Associate of the Belgian National Fund for Scientific Research.

PII S0169-4332(96)00448-5

species displaying various stoichiometries, molecular sizes and ionic charges. This drawback can be overcome (i) by taking advantage of coordination compounds in which metal atoms are surrounded by well-defined ligand configurations, and (ii) by incorporating them on the support from an organic medium. This methodology was initiated with the association of the analogous bismuth(III) tricarboxylates ($Bi(O_2CR)_3$) and dimolybdenum(II) tetracarboxylates ($Mo_2(O_2CR)_4$) containing identical ligands (same R; R = CH_3, C_2H_5, C_6H_5) [1]. It consists in the simultaneous immobilization of both compounds on the silica surface from a dispersion of small particles in *n*-heptane, according to an appropriate stoichiometry depending on the wanted bismuth molybdate phase (α-$Bi_2Mo_3O_{12}$, β-$Bi_2Mo_2O_9$ or γ-Bi_2MoO_6). In order to valorize this approach, it is essential to check: (1) whether the molecular structure of the precursors is retained up to the calcination step and (2) whether the Bi–Mo phase formed after calcination corresponds to the one expected.

The preparation is classically controlled by techniques such as powder X-ray diffraction (XRD), infra-red spectroscopy (IR), and X-ray photoelectron spectroscopy (XPS). The first two techniques, XRD and IR, provide only bulk information and usually lack sensitivity at low total metal loading of the support. As far as XPS is concerned, the preservation of the precursors is deduced by comparing the binding energies (BEs) of Bi(III) and Mo(II) before and after deposition on silica. But as the BE value mainly depends on the oxidation state, information about eventual changes in the coordination sphere cannot be easily collected from this technique. Furthermore, in calcined samples, the BEs of Bi and Mo are almost identical in pure single (Bi_2O_3 and MoO_3) and mixed oxides (α-$Bi_2Mo_3O_{12}$, β-$Bi_2Mo_2O_9$ and γ-Bi_2MoO_6), and consequently their values do not help in determining the nature of the mixed oxide. The unique useful information in this case is the atomic ratio Bi/Mo. By comparing the experimental ratio with the theoretical one corresponding to the stoichiometry of the various bismuth molybdate phases (Bi/Mo = 0.67, 1.0 and 2.0 for α-, β- and γ-phase, respectively), one may get an idea about which phase is most probably formed, if one assumes the surface stoichiometry as being representative of the phase formed. However, the unequivocal identification of the actual mixed phase present at the surface remains impossible. Therefore, new surface analysis techniques, especially those which can provide molecular information, are needed for the monitoring of the above preparation.

Time-of-flight secondary ion mass spectrometry (TOF SIMS) is a new surface technique which is based on the interaction between ions (Ga, Cs, etc.) and the material to be analyzed. In TOF SIMS experiments, short pulses of ions bombard the surface of the material and the secondary ions emitted from the surface are first accelerated to a given kinetic energy, then passed through a field-free flight tube to the detector. These secondary ions are mass-analyzed according to their flight-time. Compared with XPS, TOF SIMS offers two main advantages: (1) richer molecular information and (2) higher surface sensitivity. TOF SIMS has proven to be powerful for providing molecular information especially for organic and biological materials [2–4] and sometimes for inorganic materials [5]. However, very few studies used TOF SIMS, or even static SIMS, to characterize catalysts [6,7]. Our recent works have shown that TOF SIMS provides direct information about the surface chemistry of electrocatalysts prepared from organometallic compounds [8,9].

The objective of this work is thus to look at the potential applicability of this technique in monitoring the various stages of the above catalyst preparation. More precisely, can TOF SIMS give information about: (1) the preservation of the precursors before calcination, (2) the nature of the phases formed after calcination and (3) the dispersion of the active phase on silica? To answer the first question, the pure precursors, bismuth(III) triacetate/tribenzoate and dimolybdenum tetraacetate/tetra-benzoate, and the same precursors deposited on silica are analyzed by TOF SIMS. For the second point, the TOF SIMS spectra of the precursors deposited on silica after calcination are compared with those of pure α-

Fig. 1. Positive TOF SIMS spectra obtained with bismuth benzoate ($Bi(OBz)_3$), molybdenum benzoate ($Mo_2(OBz)_4$) and both precursors deposited on silica before calcination.

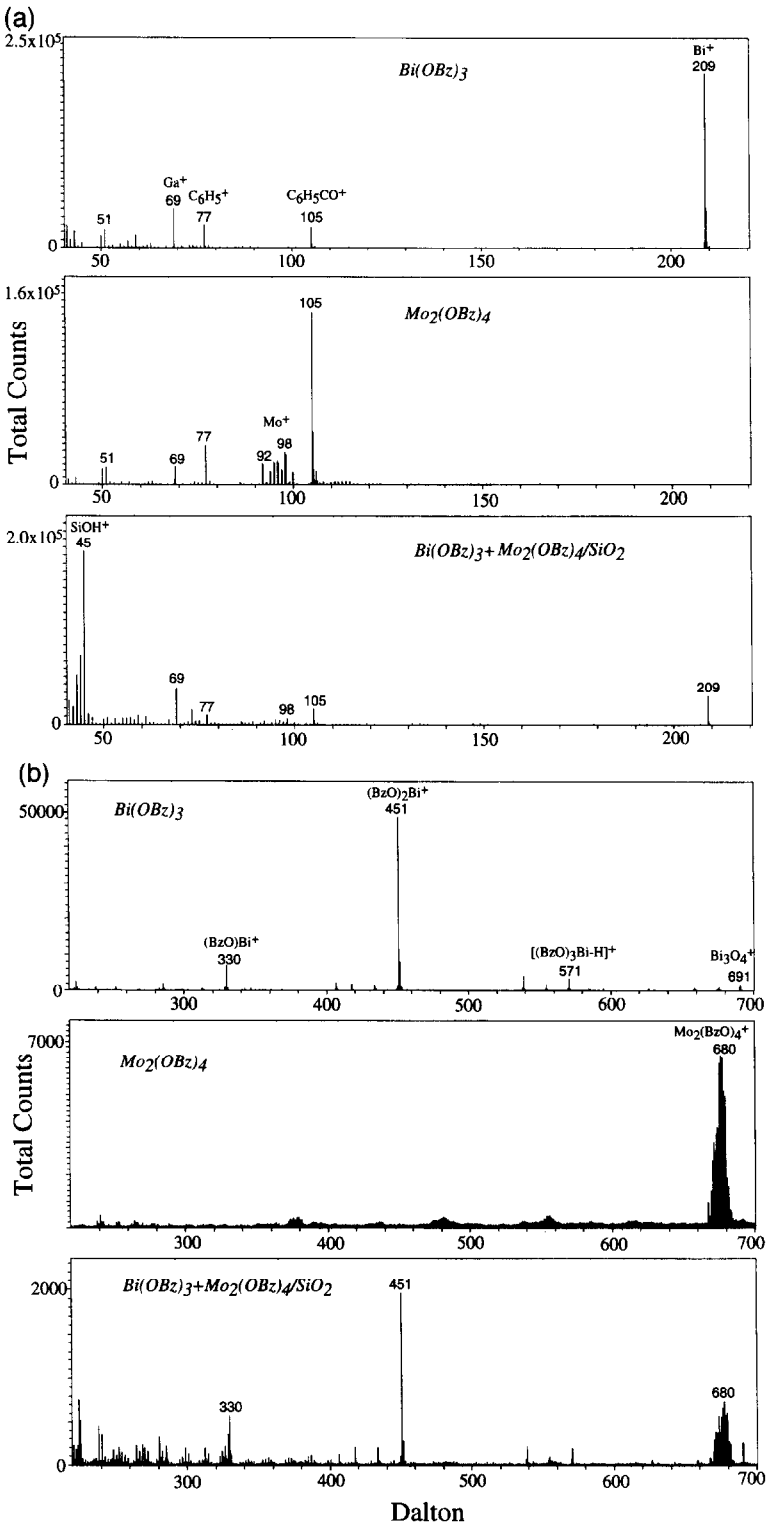
(a)
2.5x10^5
Bi(OBz)3
Bi+
209
Ga+
69
C6H5+
77
C6H5CO+
105
51
0
50
100
150
200
1.6x10^5
Mo2(OBz)4
105
Mo+
98
77
92
51
69
Total Counts
2.0x10^5
Bi(OBz)3+Mo2(OBz)4/SiO2
SiOH+
45
69
77
98
105
209
(b)
50000
Bi(OBz)3
(BzO)2Bi+
451
(BzO)Bi+
330
[(BzO)3Bi-H]+
571
Bi3O4+
691
7000
Mo2(OBz)4
Mo2(BzO)4+
680
2000
Bi(OBz)3+Mo2(OBz)4/SiO2
451
330
680
300
400
500
600
700
Dalton

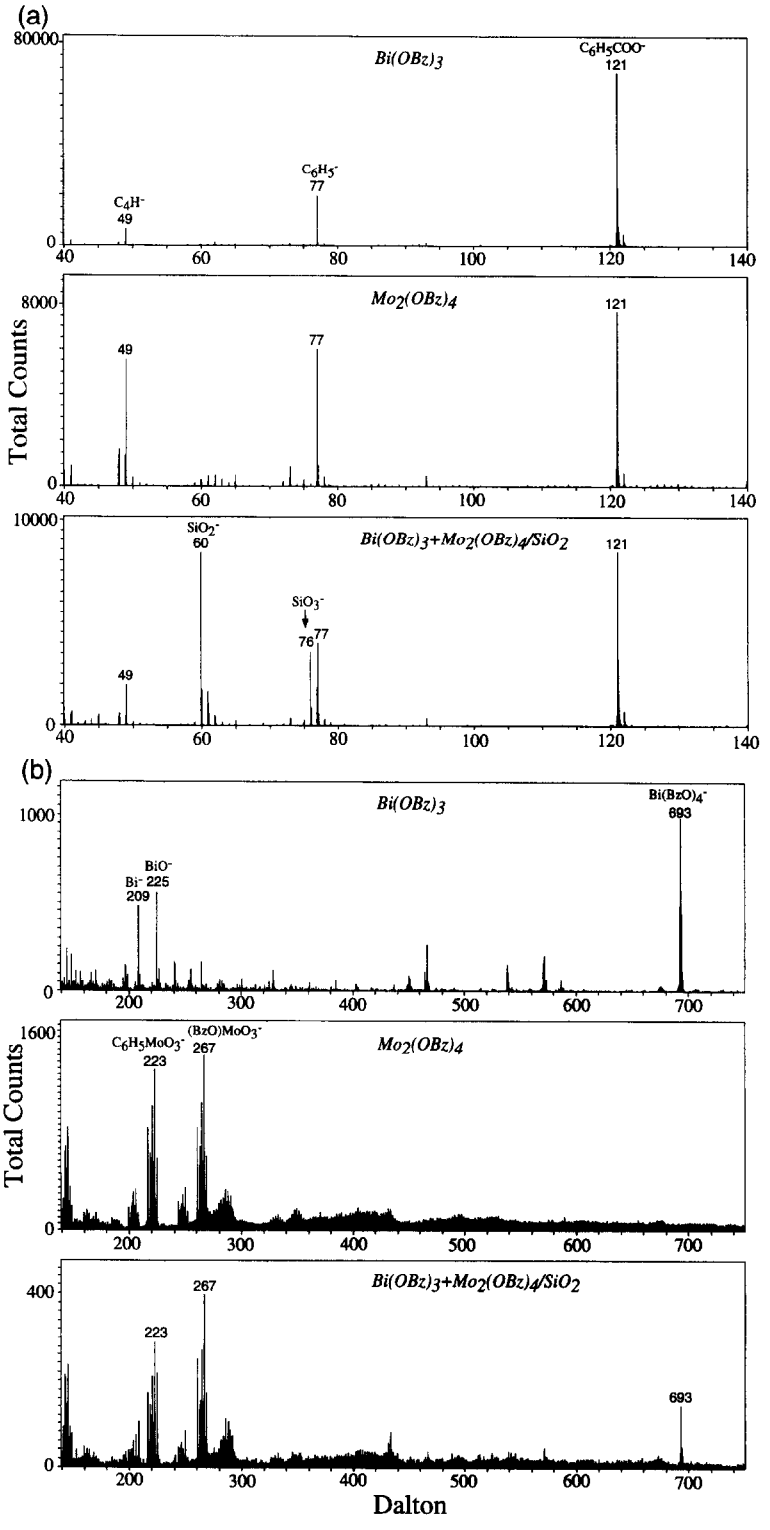
(a)
Bi(OBz)3
C6H5COO-
121
C6H5-
77
C4H-
49
Mo2(OBz)4
121
77
49
Bi(OBz)3+Mo2(OBz)4/SiO2
SiO2-
60
SiO3-
76
77
49
121
Total Counts
(b)
Bi(OBz)3
Bi(BzO)4-
693
BiO-
Bi- 225
209
Mo2(OBz)4
C6H5MoO3-
223
(BzO)MoO3-
267
Bi(OBz)3+Mo2(OBz)4/SiO2
267
223
693
Total Counts
Dalton

$Bi_2Mo_3O_{12}$, β-$Bi_2Mo_2O_9$ and γ-Bi_2MoO_6. For the last point, the characteristic secondary ions of bismuth molybdate and silica are imaged.

2. Experimental

2.1. Preparation of samples

The preparation procedures of bismuth(III) triacetate ($Bi(O_2CCH_3)_3$, noted $Bi(OAc)_3$) and dimolybdenum(II) tetraacetate ($Mo_2(O_2CCH_3)_4$, noted $Mo_2(OAc)_4$) were reported elsewhere [1]. The corresponding benzoate-type compounds, $Bi(O_2CC_6H_5)_3$ (noted $Bi(OBz)_3$), and $Mo_2(O_2CC_6H_5)_4$ (noted $Mo_2(OBz)_4$) were obtained according to similar procedures by replacing acetic acid and acetic anhydride by the benzoic analogues. The experimental details of the incorporation procedure of these precursors on silica are described in Ref. [1]. The obtention of pure single and mixed oxide phases: α-Bi_2O_3, MoO_3, α-$Bi_2Mo_3O_{12}$, β-$Bi_2Mo_2O_9$ and γ-Bi_2MoO_6 from the acetate-type precursors was reported in reference [10]. Three silica-supported samples were analyzed after thermal decomposition of the deposited precursors upon calcination: (1) sample A was prepared from acetate precursors, with 2 mol% of metal loading ((Bi + Mo)/Si = 0.02; Bi/Mo = 0.67), and calcined at 400°C; (2) sample B was obtained from acetate precursors, with 5 mol% of metal loading ((Bi + Mo)/Si = 0.05; Bi/Mo = 0.67) and calcined at 500°C; (3) sample C was prepared from benzoate precursors, with 5 mol% of metal loading ((Bi + Mo)/Si = 0.05; Bi/Mo = 2) and calcined at 500°C.

2.2. TOF SIMS measurements

Positive and negative TOF SIMS measurements were performed with a TOF SIMS spectrometer from Charles Evans & Associates [11,12]. In the TOF SIMS experiments, the sample was bombarded with pulsed Ga^+ ions (15 keV). The secondary ions were accelerated to ± 3 keV by applying a bias on the sample. The spreading of the initial energies of the secondary ions is compensated by deflection in three electrostatic analyzers. In order to increase the detection efficiency of high-mass ions, a post-acceleration of 10 kV is applied before the entry of the detector. The analyzed area used in this work is a square of 100 μm × 100 μm. With a data acquisition time of 10 min, the total ion dose is about 10^{12} ions/cm^2, which is lower than the usually accepted dose for static conditions [13]. Charge effects were compensated by means of a pulsed electron flood-gun (E_k = 20 eV). For the powder samples analyzed in this work, a stainless steel grid (non-magnetic) with an opening of 2 mm was put onto the sample surface in order to prevent variations of the surface potential. The data acquisition and treatments were made using the software developed by Charles Evans & Associates [11]. The best mass resolution obtained with this TOF SIMS spectrometer is $M/\Delta M \approx 11000$ at mass 28 amu on a Si wafer. For the samples and conditions used in this study, the mass resolution is about 3000 at 29 amu. This highly facilitates the assignment of ions having the same nominal mass but different compositions, e.g. hydrocarbon, oxygenated, nitrogen-containing fragments, etc.

The powders were pressed on an indium foil previously cleaned by ultrasonication in isopropyl alcohol. The amount of powder was adjusted to keep the layer thickness as small as possible (in order to facilitate the surface potential control during TOF SIMS analysis) but large enough to prevent detection of the substrate by TOF SIMS.

3. Results and discussion

3.1. Uncalcined samples

3.1.1. Samples prepared from Bi(III) and Mo(II) benzoate-type precursors

Figs. 1 and 2 present respectively the positive and negative spectra of pure $Bi(OBz)_3$, $Mo_2(OBz)_4$ and both precursors deposited on silica with 5 mol% of metal loading. They display the masses from 40 to 700 Da for the positive spectra and from 40 to 750

Fig. 2. Negative TOF SIMS spectra obtained with bismuth benzoate ($Bi(OBz)_3$), molybdenum benzoate ($Mo_2(OBz)_4$) and both precursors deposited on silica before calcination.

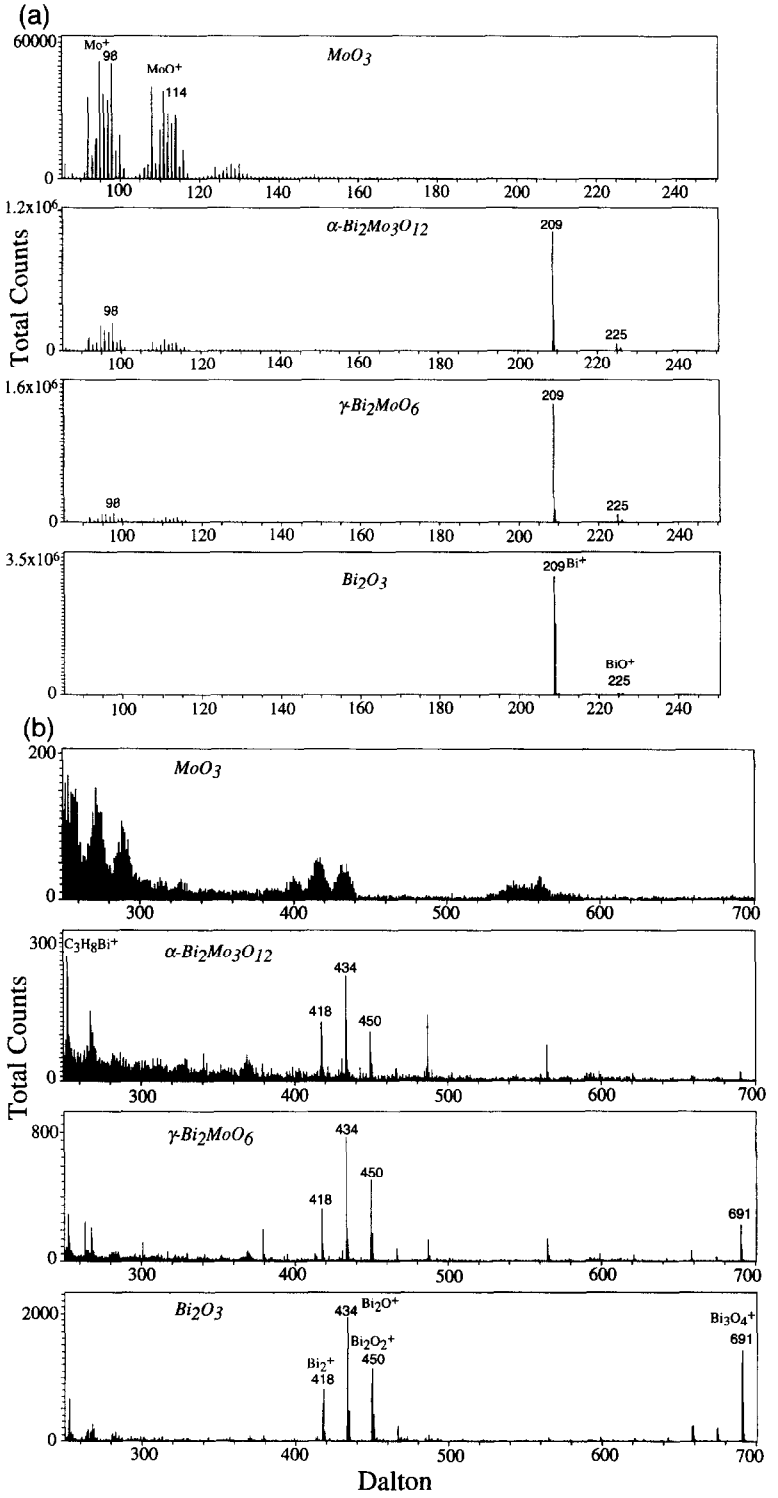
(a)
MoO3
Mo+
98
MoO+
114
α-Bi2Mo3O12
209
98
225
γ-Bi2MoO6
209
98
225
Bi2O3
209Bi+
BiO+
225
Total Counts
(b)
MoO3
C3H8Bi+
α-Bi2Mo3O12
434
418
450
γ-Bi2MoO6
434
450
418
691
Bi2O3
434
Bi2O+
Bi2O2+
450
Bi2+
418
Bi3O4+
691
Dalton

Table 1
Intense peaks observed in the positive and negative spectra of pure $Bi(OAc)_3$, $Mo_2(OAc)_4$ and both precursors deposited on silica

Samples	Positive ions	Negative ions
$Bi(OAc)_3$	$C_2H_3O^+$, Bi^+, $Bi(OAc)^+$, $Bi(OAc)_2^+$	CH_3COO^-, BiO^-, BiO_2^-, $Bi(OAc)^-$, $(Bi(OAc)_3-H)^-$, $Bi(OAc)_4^-$
$Mo_2(OAc)_4$	$C_2H_3O^+$, Mo^+, $Mo_2(OAc)_3^+$, $Mo_2(OAc)_4^+$	CH_3COO^-, MoO_2^-, MoO_3^-, $MoO_3(OAc)^-$, $Mo_2O_5^-$
$Bi(OAc)_3 + Mo_2(OAc)_4/SiO_2$	Si^+, $C_2H_3O^+$, $SiOH^+$, Mo^+, Bi^+, $Bi(OAc)^+$, $Bi_2(OAc)_3^+$, $Mo_2(OAc)_3^+$, $Mo_2(OAc)_4^+$	SiO^-, CH_3COO^-, SiO_2^-, SiO_3^-, MoO_2^-, MoO_3^-, $MoO_3(OAc)^-$, $Bi(OAc)^-$, $(Bi(OAc)_3-H)^-$, $Bi(OAc)_4^-$

Da for the negative spectra. The assignment of some important fragments is also indicated.

The positive spectrum of $Bi(OBz)_3$ (Fig. 1, top spectrum) can be easily interpreted: 571 Da (deprotonated molecular ion $(M-H)^+$), 451 Da ($Bi(OBz)_2^+$), 330 Da ($Bi(BzO)^+$), 209 Da (Bi^+), 105 Da ($C_6H_5CO^+$) and 77 Da ($C_6H_5^+$). Its negative spectrum is dominated by O^- and OH^- (not shown). In the mass range 40–140 Da (Fig. 2, top spectrum), we observe C_4H^-, $C_6H_5^-$ and $C_6H_5COO^-$ and the mass range 140–750 Da is dominated by a peak at 693 Da, corresponding to $Bi(OBz)_4^-$.

Similarly, the most intense peaks in the positive spectrum of $Mo_2(OBz)_4$ (Fig. 1, central spectrum) can be assigned as follows: 680 Da (molecular ion $Mo_2(OBz)_4^+$), 105 Da ($C_6H_5CO^+$), 98 Da (Mo^+) and 77 Da ($C_6H_5^+$). As Mo has isotopes from 92 to 100 Da, the molecular ion is in fact a cluster from 668 to 684 Da. The negative spectrum of $Mo_2(OBz)_4$ is also dominated by the low-mass ions: O^-, OH^-, etc. (not shown). In the mass range 40–140 Da, we observe the same fragments as for $Bi(OBz)_3$: C_4H^-, $C_6H_5^-$, $C_6H_5COO^-$. Beyond mass 140 Da, we observe two important fragments: $C_6H_5MoO_3^-$ and $(BzO)MoO_3^-$. However, no negative molecular ion is observed in this case.

The positive and negative spectra obtained with the precursors deposited on silica (Figs. 1 and 2, bottom spectra) can be considered as the combination of those of pure $Bi(OBz)_3$, $Mo_2(OBz)_4$ and SiO_2 (not shown). In the positive spectrum (Fig. 1, bottom spectrum), except for Si^+ (not shown) and $SiOH^+$ from SiO_2, the spectrum is dominated by the molecular ions and the most characteristic fragments of the both precursors. The same conclusion can be drawn from the negative spectrum (Fig. 2, bottom spectrum). These results clearly show that the precursors are preserved on the surface of silica before calcination.

3.1.2. Samples prepared from Bi(III) and Mo(II) acetate-type precursors

In a similar way, pure $Bi(OAc)_3$, $Mo_2(OAc)_4$ and both precursors deposited on silica were analyzed in TOF SIMS and their spectra were compared. Table 1 summarizes some intense peaks detected in the three samples. It can be observed that the molecular ions and most characteristic fragments of both precursors are undoubtedly present in the spectra of the silica samples loaded with these precursors. This confirms that the molecular structure of the precursors is retained when they are deposited on silica.

The results obtained with the above two systems clearly show that, through the observation of the molecular ions and most characteristic fragments of the precursors, TOF SIMS provides direct information about the preservation of precursors when they are deposited on silica.

3.2. Calcined samples

3.2.1. Pure bismuth molybdates

In order to see whether TOF SIMS is able to distinguish between different bismuth molybdate

Fig. 3. Positive TOF SIMS spectra obtained with MoO_3, α-$Bi_2Mo_3O_{12}$, γ-Bi_2MoO_6 and Bi_2O_3.

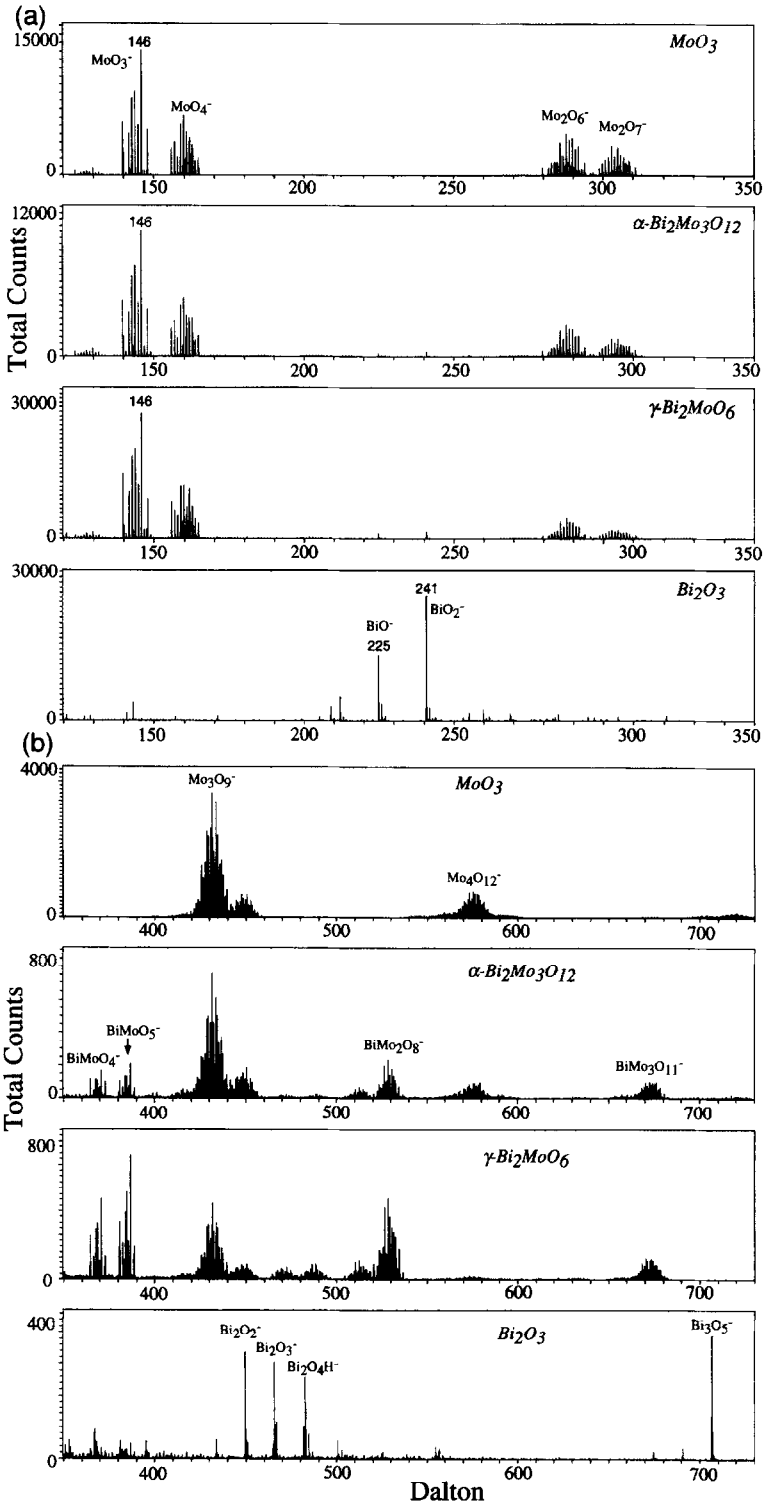
(a)
MoO3
146
MoO3-
MoO4-
Mo2O6-
Mo2O7-
α-Bi2Mo3O12
γ-Bi2MoO6
Bi2O3
241
BiO2-
BiO-
225
(b)
Mo3O9-
Mo4O12-
BiMoO5-
BiMoO4-
BiMo2O8-
BiMo3O11-
Bi2O2-
Bi2O3-
Bi2O4H-
Bi3O5-
Total Counts
Dalton

phases, we first analyzed the three pure bismuth molybdate phases prepared from Bi(III) and Mo(II) acetate-type precursors, α-$Bi_2Mo_3O_{12}$, β-$Bi_2Mo_2O_9$ and γ-Bi_2MoO_6. For comparison, the two related single oxides, Bi_2O_3 and MoO_3, were also examined.

Figs. 3 and 4 show respectively the positive and negative spectra for MoO_3, α-$Bi_2Mo_3O_{12}$, γ-Bi_2MoO_6 and Bi_2O_3. The investigated masses range from 90 to 700 Da for the positive spectra and from 125 to 730 Da for the negative spectra. The TOF SIMS spectra of β-$Bi_2Mo_2O_9$ are similar to those of α-$Bi_2Mo_3O_{12}$ and γ-Bi_2MoO_6 and are not included in the figures. The assignment of some intense and characteristic peaks is also indicated.

The comparison of these spectra shows that:

(1) In the positive spectra (Fig. 3), except for a group of peaks around 837 Da which can be assigned as $Bi_3MoO_7^+$ (not shown), all the peaks found in the mixed phases are present either in the spectrum of MoO_3 or in the spectrum of Bi_2O_3. Moreover, all three mixed oxide phases show the same fragments. In other words, there are no fragments that can be considered as characteristic of each phase. However, the relative SIMS intensity of these fragments are different (see below). Compared with pure Bi_2O_3, the intensity of $Bi_3O_4^+$ decreases significantly in the mixed phases ($Bi_3O_4^+/Bi^+$ is about 0.006 in Bi_2O_3 while only 0.002 in γ-Bi_2MoO_6 and 0.0003 in α-$Bi_2Mo_3O_{12}$). It has to be noted that the peaks at 487 and 565 Da seen only on the pure bismuth molybdate phases are attributed to compounds associating bismuth oxide and hydrocarbon ($BiO_xC_yH_z$), there exact identification is however difficult.

(2) Similarly, in the negative spectra (Fig. 4), most of the fragments present in the mixed phases are detected either in the spectrum of MoO_3, or in the spectrum of Bi_2O_3. But several fragments in the mass range 350–730 Da can be assigned to the association between MoO_3 and Bi_2O_3: $BiMoO_4^-$, $BiMoO_5^-$, $BiMo_2O_8^-$ and $BiMo_3O_{11}^-$. Again, the three mixed phases show the same fragments but their intensities are different. Interestingly, some high-mass fragments of Bi_2O_3 are totally absent in the spectra of the mixed phases: $Bi_2O_2^-$, $Bi_2O_3^-$, $Bi_2O_4H^-$ and $Bi_3O_5^-$. Thus, the occurrence of these ions may be used as fingerprint for the presence of Bi_2O_3.

These results show that it is not possible to distinguish between the three mixed phases by referring only to their TOF SIMS fragmentation patterns. It should be noted that the obtention of identical fragments for these phases in both the positive and the negative spectra is in total agreement with the fact that these phases differ only in the organization of stacked Bi- and Mo-layers. On the other hand, the presence of increased amounts of Mo-layers in the mixed phases would inhibit the production of the Bi-containing ions at high mass. This may account for the intensity decrease of $Bi_3O_4^+$ when going from pure Bi_2O_3 to the γ-phase and further to the α-phase, and for the absence of $Bi_3O_5^-$ in the spectra of the mixed phases.

There remains one possibility to see whether TOF SIMS is able to distinguish between these phases, i.e. the comparison of the SIMS intensity of certain fragments. For that purpose, the intensities of the positive and negative ions are normalized respectively to those of Mo^+ and MoO_3^- (the most intense Mo-containing ions in the spectra). The so calculated intensity ratios, X^+/Mo^+ and X^-/MoO_3^-, are then compared with the bulk Bi/Mo ratio. For the positive spectra, the following intensity ratios are found to be linearly related to the bulk Bi/Mo ratio: Bi^+/Mo^+, BiO^+/Mo^+, Bi_2^+/Mo^+, Bi_2O^+/Mo^+ and $Bi_2O_2^+/Mo^+$. As an example, Fig. 5 illustrates the relationship between $Bi_2O_2^+/Mo^+$ and the bulk Bi/Mo ratio. Similar correlations were, however, not found for the negative spectra. These results show that, despite the similarities between their SIMS fragmentation patterns, the three pure bismuth molybdates can, nevertheless, be distinguished in an indirect manner by comparing the SIMS intensity ratios of certain positive fragments.

3.2.2. Calcined samples prepared from acetate and benzoate-type precursors

As indicated in the experimental section, three samples (sample A, B and C) were analyzed by TOF

Fig. 4. Negative TOF SIMS spectra obtained with MoO_3, α-$Bi_2Mo_3O_{12}$, γ-Bi_2MoO_6 and Bi_2O_3.

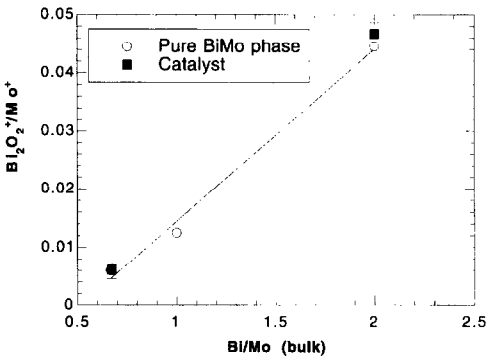

Fig. 5. SIMS intensity ratio $Bi_2O_2^+/Mo^+$ as a function of bulk Bi/Mo ratio obtained with pure bismuth molybdate phases and with catalysts (samples B and C).

SIMS. The Bi and Mo contents of samples A and B were selected in order to produce the α-phase, while the two metals were incorporated according to the stoichiometry of the γ-phase in sample C. Sample A was calcined at 400°C, while samples B and C were calcined at 500°C.

The positive and negative TOF SIMS spectra obtained with these three samples (not shown) are similar to those of the pure bismuth molybdate phases except for some ions from SiO2 (Si^+, $SiOH^+$ etc. in the positive and SiO^- and SiO_2^-, SiO_3^- in the negative spectra). In order to see whether the bismuth molybdate phases formed on the surface of SiO_2 correspond to those expected, some SIMS intensity ratios from the positive spectra are calculated and compared with those obtained with the pure bismuth molybdate phases. The results for samples B and C are summarized in Table 2 (the $Bi_2O_2^+/Mo^+$ values for these two samples are also indicated in Fig. 5). It can be observed that the SIMS intensity ratios obtained with these two samples are reproducible (in most cases deviation being lower than 10%). By comparing these intensity ratios with those characterizing the pure phases, one can conclude that:

(1) for sample B, except for the ratio BiO^+/Mo^+ which is slightly higher, all the SIMS intensity ratios are very close to those of pure α-$Bi_2Mo_3O_{12}$. By taking into account the fact that α-$Bi_2Mo_3O_{12}$ phase was detected by XRD in the bulk and that the Bi/Mo ratio determined by XPS was 0.6 (i.e. close to the stoichiometric one), these results strongly suggest that α-$Bi_2Mo_3O_{12}$ is formed in sample B.

(2) similarly, for sample C, most of the SIMS intensity ratios are close to those of pure γ-Bi_2MoO_6 (except again for the ratio Bi^+/Mo^+ which is slightly higher). In agreement with the XRD results and with the Bi/Mo ratio observed in XPS (Bi/Mo = 1.64), this indicates that the γ-phase is formed in sample C.

It should be recognized that this approach is similar to the use of the XPS Bi/Mo atomic ratio. However, as pointed out in the introduction, the use of intensity ratio(s) is not a direct way for the identification of a mixed phase. Indeed, finding for an unknown sample the same intensity ratio(s) as for the pure mixed phase cannot be taken as a guaranty for the formation of that phase. This is only a indication that has to be confirmed by other techniques, as we did above for the silica supported Bi–Mo samples.

In order to look at the dispersion of bismuth molybdate phases in samples B and C, the secondary ions characteristic of bismuth molybdate and silica are imaged respectively. Fig. 6 shows three typical images taken respectively with Si^+, $Mo^+ + MoO^+$ and Bi^+ for sample B. It can be observed that for most of the regions, both Bi and Mo are homogeneously distributed in SiO_2. But some spots of Bi and Mo (about 10–15 μm in diameter) are observed.

Table 2
Comparison of some positive SIMS intensity ratios between pure bismuth molybdates and samples prepared from acetate or benzoate-type precursors after calcination

Intensity ratio	α-$Bi_2Mo_3O_{12}$	Sample B	γ-Bi_2MoO_6	Sample C
Bi^+/Mo^+	4.57 ± 0.19	4.26 ± 0.41	11.24 ± 0.29	15.48 ± 0.98
BiO^+/Mo^+	0.276 ± 0.018	0.382 ± 0.035	0.823 ± 0.040	0.762 ± 0.063
Bi_2^+/Mo^+	0.00739 ± 0.00052	0.0083 ± 0.0021	0.0293 ± 0.0016	0.0362 ± 0.0044
Bi_2O^+/Mo^+	0.0113 ± 0.0005	0.0111 ± 0.0024	0.0639 ± 0.0040	0.0773 ± 0.0047
$Bi_2O_2^+/Mo^+$	0.00603 ± 0.00056	0.00613 ± 0.00140	0.0446 ± 0.0020	0.0467 ± 0.0040

They correspond to aggregates of the bismuth molybdate phase. Similar results were obtained with sample C.

For sample A (calcined at 400°C), however, the SIMS intensity ratios change from one analyzed region to another. For example, Bi^+/Mo^+ changes from 2.0 for one region to 5.3 for another. This indicates that Bi and Mo are not homogeneously dispersed in SiO_2. This can be further seen from the images presented in Fig. 7. Indeed, on the up-right side of the images, we observe only Bi signal with almost no signal from Mo. This indicates that this 'Bi-rich' region may be due to the presence of either pure Bi_2O_3 or a bismuth molybdate phase rich in Bi (e.g. γ-phase), or even a mixture of them. As the XRD patterns revealed the presence, in this sample, of the α-phase together with trace amounts of the γ-phase, it is likely that this 'Bi-rich' region corresponds to a surface enrichment in the γ-phase. The

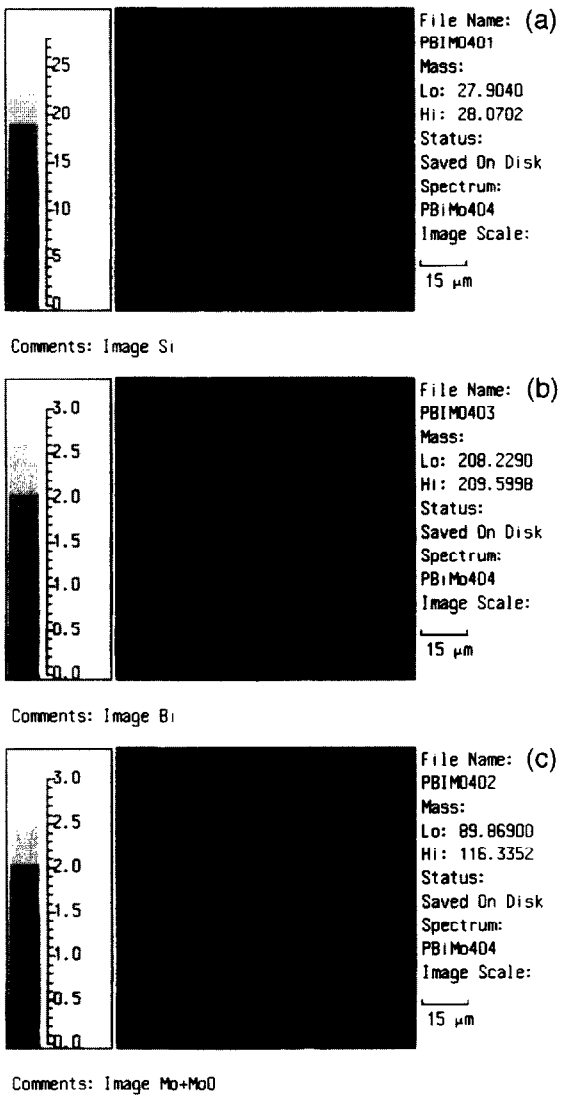

Fig. 6. TOF SIMS images obtained with catalyst sample B. Images taken from (a) Si^+; (b) Bi^+ and (c) $Mo^+ + MoO^+$.

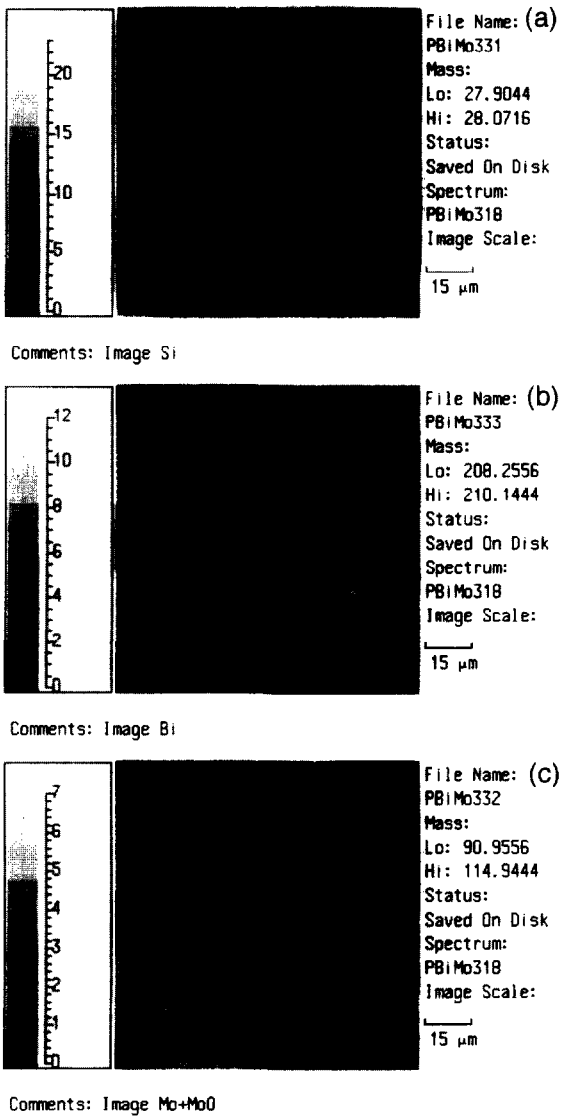

Fig. 7. TOF SIMS images obtained with catalyst sample A. Images taken from (a) Si^+; (b) Bi^+ and (c) $Mo^+ + MoO^+$.

SIMS results suggest that sample A is not a pure phase but a mixture of phases. On the other hand, the comparison between Figs. 6 and 7 shows that the bismuth molybdate aggregates in sample A are much larger than those in samples B and C. This suggests that the dispersion of bismuth molybdates is worse in sample A, in line with the fact that the calcination temperature for this sample was lower.

4. Conclusions

Several conclusions can be drawn from the present work:

(1) TOF SIMS can provide direct information about the preservation of the molecular structure of coordination compounds after their deposition on silica. This is achieved by the observation of the molecular ions and most characteristic fragments of the coordination compounds.

(2) As TOF SIMS shows the same characteristic fragments for the three pure bismuth molybdate phases (α, β and γ), these phases cannot be distinguished directly from their fragmentation patterns. This makes the identification of the mixed phases more difficult. However, the three pure phases differ in SIMS intensity ratios. In particular, it has been shown that the SIMS intensity ratios, Bi^+/Mo^+, BiO^+/Mo^+, Bi_2^+/Mo^+, Bi_2O^+/Mo^+ and $Bi_2O_2^+/Mo^+$, are linearly related to the bulk Bi/Mo ratios. Therefore, these intensity ratios can be used for the identification of a mixed phase. Indeed, we have applied this method to determine the nature of bismuth molybdate phases formed on the silica surface. This approach is somehow similar to the use of the Bi/Mo atomic ratios determined by XPS. However, one advantage of TOF SIMS over XPS lies in its higher sensitivity.

(3) TOF SIMS imaging has been shown to be very useful for providing information about the dispersion of bismuth molybdate on silica.

Acknowledgements

The financial support from the "Fonds National de la Recherche Scientifique (F.N.R.S.)-Loterie Nationale" (Belgium) and the "Région Wallonne" (Belgium) for the purchase of our TOF SIMS spectrometer, and the "Institut pour l'Encouragement de la Recherche dans l'Industrie et l'Agriculture" (I.R.S.I.A., Brussels) for the fellowship allotted to O. Tirions, are gratefully acknowledged.

References

[1] O. Tirions, M. Devillers, P. Ruiz and B. Delmon, in: Preparation of Catalysts VI, Eds. G. Poncelet et al. (Elsevier, Amsterdam, 1995) p. 999.
[2] J.C. Vickerman, Analyst 119 (1994) 513.
[3] A. Benninghoven, Angew. Chem. Int. Ed. Engl. 33 (1994) 1023.
[4] D. Briggs, in: Practical Surface Analysis, Vol. 2, Ion and Neutral Spectroscopy, Eds. D. Briggs and M.P. Seah (Wiley, Chichester, 1990) p. 367.
[5] N.M. Reed, J.C. Vickerman and D. Briggs, in: Practical Surface Analysis, Vol. 2, Ion and Neutral Spectroscopy, Eds. D. Briggs and M.P. Seah (Wiley, Chichester, 1990) p. 303.
[6] Y. Zhou, M.C. Wood and N. Winograd, J. Catal. 146 (1994) 82.
[7] Y.S. Jin, Q.J. Yan, Z.R. Yin and Y. Chen, J. Chem. Soc. Faraday Trans. 91 (1995) 381.
[8] L.T. Weng, P. Bertrand, G. Lalande, D. Guay and J.P. Dodelet, Appl. Surf. Sci. 84 (1995) 9.
[9] G. Lalande, R. Côté, G. Tamizhmani, D. Guay, J.P. Dodelet, L. Dignard-Bailey, L.T. Weng and P. Bertrand, Electrochim. Acta 40 (1995) 2635.
[10] M. Devillers, O. Tirions, L. Cadus, P. Ruiz and B. Delmon, submitted.
[11] B. Schueler, P. Sander and D.A. Reed, Vacuum 41 (1990) 1661.
[12] B. Schueler, Microsc. Microanal. Microstruct. 3 (1992) 119.
[13] D. Briggs and M.J. Hearn, Vacuum 36 (1986) 1005.